Journal of Innovative Optical Health Sciences
Vol. 11, No. 5 (2018) 1850031 (15 pages)

DOI: 10.1142/S1793545818500311

Evaluation of growth characteristics of *Aspergillus parasiticus* inoculated in different culture media by shortwave infrared (SWIR) hyperspectral imaging

Xuan Chu[*,†], Wei Wang[*,§§], Xinzhi Ni[‡], Haitao Zheng[§], Xin Zhao[*], Hong Zhuang[¶], Kurt C. Lawrence[‖], Chunyang Li[**], Yufeng Li[††,¶¶] and Chengjun Lu[‡‡]

[*]*College of Engineering, China Agricultural University*
Beijing 100083, P. R. China

[†]*College of Mechanical and Electrical Engineering*
Zhongkai University of Agriculture Engineering
Guangzhou 510225, P. R. China

[‡]*Crop Genetics and Breeding Research Unit*
USDA-ARS, 2747 Davis Road, Tifton, GA 31793, USA

[§]*College of Food Science & Nutritional Engineering*
China Agricultural University, Beijing 100083, P, R. China

[¶]*Quality & Safety Assessment Research Unit*
U.S. National Poultry Research Center, USDA-ARS
950 College Station Rd., Athens, GA 30605, USA

[‖]*Quality & Safety Assessment Research Unit*
USDA-ARS, Athens, GA 30605, USA

[**]*Institute of Food Science and Technology*
Jiangsu Academy of Agricultural Sciences
Nanjing 210014, P. R. China

[††]*Multidisciplinary Initiative Center*
Institute of High Energy Physics
Chinese Academy of Sciences
Beijing 100049, P. R. China

[‡‡]*Lingang Experimental Middle School*
Linyi 276624, P. R. China
[§§]*playerwxw@cau.edu.cn*
[¶¶]*liyf@ihep.ac.cn*

[§§,¶¶]Corresponding authors.

Received 15 March 2018
Accepted 13 August 2018
Published 12 September 2018

The growth characteristics of *Aspergillus parasiticus* incubated on two culture media were examined using shortwave infrared (SWIR, 1000–2500 nm) hyperspectral imaging (HSI) in this work. HSI images of the *A. parasiticus* colonies growing on rose bengal medium (RBM) and maize agar medium (MAM) were recorded daily for 6 days. The growth phases of *A. parasiticus* were indicated through the pixel number and average spectra of colonies. On score plot of the first principal component (PC_1) and PC_2, four growth zones with varying mycelium densities were identified. Eight characteristic wavelengths (1095, 1145, 1195, 1279, 1442, 1655, 1834 and 1929 nm) were selected from PC_1 loading, average spectra of each colony as well as each growth zone. Furthermore, support vector machine (SVM) classifier based on the eight wavelengths was built, and the classification accuracies for the four zones (from outer to inner zones) on the colonies on RBM were 99.77%, 99.35%, 99.75% and 99.60% and 99.77%, 99.39%, 99.31% and 98.22% for colonies on MAM. In addition, a new score plot of PC_2 and PC_3 was used to differentiate the colonies incubated on RBM and MAM for 6 days. Then characteristic wavelengths of 1067, 1195, 1279, 1369, 1459, 1694, 1834 and 1929 nm were selected from the loading of PC_2 and PC_3. Based on them, a new SVM model was developed to differentiate colonies on RBM and MAM with accuracy of 100.00% and 99.99%, respectively. In conclusion, SWIR hyperspectral image is a powerful tool for evaluation of growth characteristics of *A. parasiticus* incubated in different culture media.

Keywords: *Aspergillus parasiticus*; growth characteristics; characteristic wavelengths; shortwave infrared (SWIR) hyperspectral imaging.

1. Introduction

Fungi are a group of microorganisms with great environmental significance, especially in food safety.[1] They grow almost everywhere under most conditions and can cause food spoilage. Certain strains of fungi even produce life-threatening toxins to humans and livestock, such as aflatoxin produced by *Aspergillus flavus* and *Aspergillus parasiticus*, and fumonisins produced by *Fusarium moniliforme* and *Fusarium proliferatum*.[2,3] Studying growth characteristics of fungi especially during its spore germination would help to prevent saprophytic degradation and mycotoxins accumulating.

Before detecting fungi in real food materials directly, exploring fungal growth on agar medium to obtain phenotypic characters of pure isolates of fungi is the general way. The traditional methods to describe fungal growth were mainly based on the measurement of morphological features, total viable count,[4] biomass,[5] texture and microscopic structure of colonies, metabolite production concentrations[6] and resource uptake.[7] The model consisted of partial differential equations for accumulation of hyphae by apical growth, uptake of nutrient, and redistribution of a derived metabolite within the mycelium. These traditional microbiological measurement methods in modeling fungal growth are generally time consuming and require specialized instruments and trained personnel.

More recently, hyperspectral image (HSI) technique has become increasingly important for rapid and nondestructive testing for the quality and safety assessment of food and agricultural products.[8] As the hyperspectral image data is a combination of spectral and spatial information, it can be used to extract image feature at specified wavelengths, evaluate spectral information of target pixels, or analyze both spatial and spectral information at the same time.

In the past decades, hyperspectral imaging has been successfully applied for modeling growth of several varieties of fungi. Dégardin *et al.* (2015)[9] measured the growth of *A. flavus* colony using Vis/NIR HSI technique and identified spectral signatures for *A. flavus*. Results showed that the reflectance of *A. flavus* colony surface in different

growth periods were significantly different in some regions of the wavelength spectrum. Williams *et al.* (2012a, 2012b)[10,11] studied the growth characteristics and differences among the strains of *Fusarium*. However, there were still limited studies about fungal growth characteristics for other kinds of fungi by HSI technique. Some strain classifications of fungi by HSI could be treated as references. Jin *et al.* (2009)[12] classified toxigenic and atoxigenic *Aspergillus flavus* by hyperspectral image under UV light and halogen light source. Yao *et al.* (2008)[13] identified five kinds of toxigenic fungi using hyperspectral image, and the five fungi could be easily separated with accuracy of 97.7% by the wavelengths of 743, 458 and 541 nm. These cases indicated that HSI technique is a powerful tool for fungi detection.

Aspergillus parasiticus, one of the predominant aflatoxin producing *Aspergillus* species, is widely present in food and grain. Using HSI to explore its image and the spectral characteristics associated with its growth process would help to achieve early detection of *A. parasiticus*. As fungal development on food products is complex, it is necessary to investigate it in a controlled manner and environment.

This study aimed at observing the growth characteristics of *A. parasiticus* incubated on two different nutritional media using shortwave infrared (SWIR) hyperspectral imaging. The specific objectives were to (1) investigate growth phases and growth zones of *A. parasiticus* colonies incubated on each of the two media for different durations, and determine their specific spectral signature; (2) acquire feature parameters and select characteristic wavelengths to identify and discriminate *A. parasiticus* incubated on different media; (3) classify varying growth zones on *A. parasiticus*colonies and *A. parasiticus* incubated on different media using the simplified support vector machine (SVM) classification models based on the spectra of selected characteristic wavelengths.

2. Materials and Methods

2.1. *Sample preparation*

A. parasiticus (strain number: CGMCC 3.6155) was obtained from China General Microbiological Culture Collection Center (CGMCC), Beijing, China. It was cultured on potato dextrose agar (PDA) tubes at 28°C for 7 days to obtain heavily sporulating cultures. The conidia of the *A. parasiticus* were removed from PDA by a sterile inoculation loop to 0.9% sterile saline to make suspension. The concentration was then adjusted to 10^6 spores mL^{-1} by a haemocytometer (Qiujing, Shanghai, China). 10 μL culture stock was introduced to the center of the rose bengal medium (RBM) and maize agar medium (MAM) Petri plates with a pipette. The inoculation was performed for 6 days with regular interval of 24 h to acquire colonies collectively. All Petri plates were incubated in an incubator at 30°C.

2.2. *Hyperspectral imaging acquisition*

A SWIR hyperspectral image system was set up for image acquisition. The system consists of a line scan spectral camera (Specim, Spectral Imaging Ltd, Oulu, Finland), a cryogenically cooled MCT detector, a 30 mm front lens (OLES30, Specim, Oulu, Finland), two halogen lamps with a power of 50 W, and a motorized linear stage (TLSR300B, Zaber Technologies, Inc., Vancouver, British Columbia, Canada). Output images contain 384 pixels in each line-scan width, and the pixel resolution of the system was 0.35 mm × 0.35 mm. Reflectance spectrum of each pixel includes 288 bands from 921 to 2529 nm at 12 nm resolution and 5.6 nm wavelength intervals. Image acquisition was performed using in-house software that controlled various imaging parameters, which were set as follows: the distance of the camera from the target was 40 cm, the lights positioned at approximately 45° angles and 35 cm above and lateral to the target, exposure time was 10 ms, and the speed of motorized translation stages was 0.35 cm/s.

White and dark current reference images were captured prior to the acquisition of each sample image and used for image correction. The dark current image data were taken with the camera shutter completely closed, and white reference image was captured by scanning a Teflon white board (99.99% reflectivity). Images of the entire Petri plates were acquired with their lids removed. These hyperspectral images were calibrated by the following equation:

$$R = \frac{R_o - R_d}{R_w - R_d} \times 100\%, \tag{1}$$

where R was the corrected reflectance spectra; R_o was the original reflectance spectra; R_w and R_d were white and dark reference reflectance spectra, respectively.

2.3. *Multivariate data analysis methods*

In this work, median filter was used to remove the noise of hyperspectral image, principal component analysis (PCA) was used to remove specific pixels of background and extract fungal growth characteristics. Two SVM classification models were developed to identify different growth zones of fungi inoculated on a specific culture medium, and to differentiate the same fungus grown on different nutritional media, respectively.

PCA projects original variables onto a set of new variables (principal components, PCs) which are orthogonal to each other and can keep maximum variation of the data points in the original spectral space.[14] In the PC space, the scores represent the weighted sums of the original variables without significant loss of useful information. PCA score plots could give an indication of clustering of groups comprised of similar pixels.[15] The coefficients multiplying each variable were called loadings, which could be adopted to explain the relationship between PCA score and characteristic wavelength.[16]

In this study, PCA was first applied on the preprocessed hyperspectral data to remove background noise and extract fungal colonies. Background components (culture media, petri dishes) were highlighted in the score image removed with the help of a mask. After fungal colonies were extracted, three mosaic images were constructed. The first and second mosaic image was composed of the hyperspectral images of colonies respectively growing on RBM and MAM for 2–6 days the third one was grouped by the hyperspectral images of two colonies incubated for 6 days respectively on RBM and MAM. It should be noted that there is no visual information and most spectral data are produced mainly by noise within the first 24 h of the initial inoculation. Perhaps during this period, fungal mycelium is in a chaotic state of spore germination. Thus, only colonies incubated for 2 to 6 days were analyzed in this work. On the background removed image, there were some bad pixel lines on images of

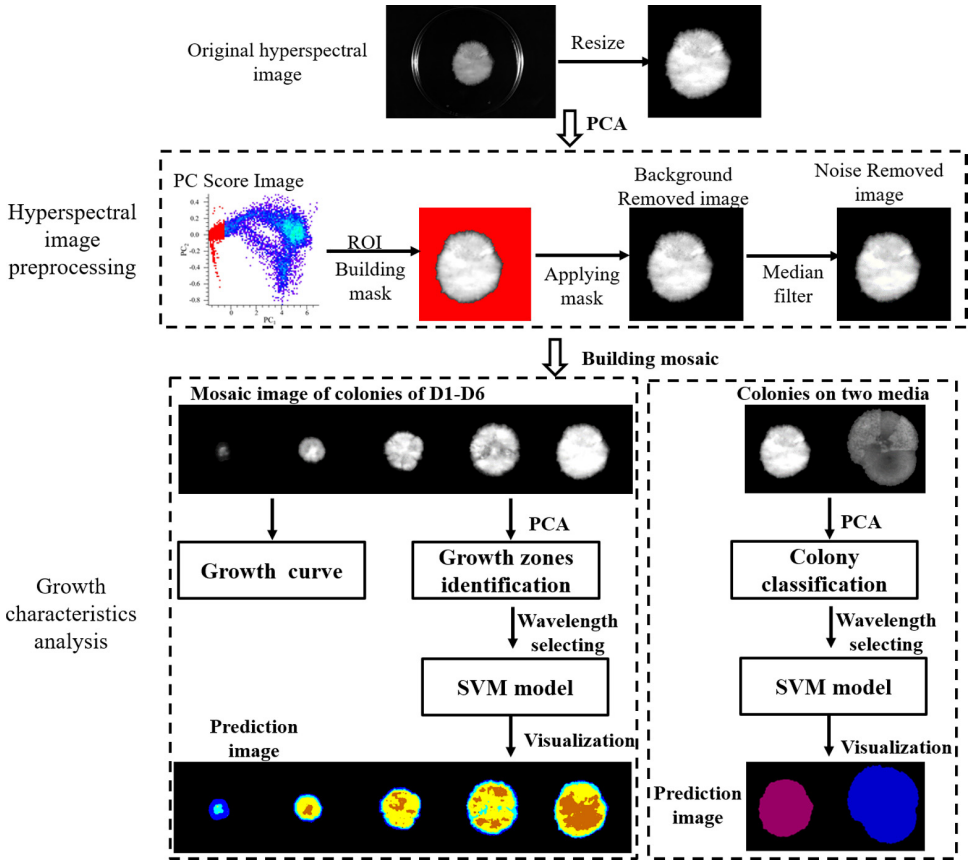

Fig. 1. Flowchart of data processing.

some bands, which were generated by the line scan result of residual isolated bad pixels of MCT detector. These bad pixel lines also lead to unusual serrated peaks on the spectra. Median filter (3 × 3 kernel) was further applied on the background removed image to correct the bad pixel lines in the spectral image. The growth characteristics of the fungus incubated on the same medium or different media could all be explained with an interactive analysis of PC score image, score plot, as well as PC loadings. Key wavelengths were also selected by the loading line plot of PCs.

SVM was widely used in classification problems, which can create a hyperplane that can make the largest classification interval between each class of samples in the higher dimension feature space.[17] In order to identify growth rings on colonies, pixel reflectance spectra at characteristic wavelengths of different zones of the colonies were served as the input of SVM classifier. The growth zones obtained by the PCs score plot method were as references. The classification performance was evaluated by comparing to the results obtained by SVM model and PCs score plot method. Similarly, identification of the fungus grown on different media was based on the selected characteristic wavelengths of each colony. The results were compared to the actual type of the colonies. Hyperspectral data analysis was carried out in ENVI 4.7 (Research System Inc., Boulder, CO, USA) and MATLAB 2013b (The Math Works, Natick, MA, USA) software environment.

2.4. *The flow-chart of data processing*

Figure 1 was the flowchart of data processing. It shows the preprocess method and the processing of proposed method to analyze growth characteristics of *A. parasiticus* and discriminate them incubated on different media.

3. Results and Discussion

3.1. *Hyperspectral image preprocessing*

Processing on hyperspectral image of colony incubated from the 2nd to 6th days on RBM was illustrated (Fig. 2). Figure 2(a) shows the colony almost grown in the center of the Petri plate and occupying only a small area. To reduce calculation to remove the region without colony, the original images were all cropped to ones with 161 × 161 pixels. The corresponding spectral range was also shortened to 1000–2200 nm, because the detector is less sensitive at the rest spectral regions (921–1000 nm and 2200–2529 nm) resulting low SNR (Signal Noise Ratio). The resultant hypercubes were 161 (W) × 161 (H) × 214 (wavelengths). Furthermore, the PCA was applied on these hypercubes. Score plot of PC_1 and PC_2 (Fig. 2(b)) was used to extract colonies. The red class in Fig. 2(b) corresponded to the background pixels shown in Fig. 2(c). It was exported using region of interest (ROI) tools in ENVI and used to make a mask to remove the background information on the resized hypercubes, and the resultant fungi image was shown in Fig. 2(d). Then median filter (3 × 3 kernels) was applied on the background removed hyperspectral image to correct the bad pixels on the image.[18] The corrected colony images were shown in Fig. 2(e). They were used to build mosaics (Figs. 2(f) and 2(g)). The first and second mosaic images comprised of the hyperspectral images of colonies, respectively, growing on RBM and MAM for 2–6 days, which subsequently were used to analyze the fungal growth characteristics. In order to analyze the *A. parasiticus* incubated on different media, the third mosaic image consisted of both colonies on RBM and MAM for 6th days, which subsequently was used to analyze the unique characteristics of fungus growing on the two media.

3.2. *Fungal growth phase and their average spectra*

A fungal spore in the range favorable conditions germinates to form hyphae.[19,20] Hyphae extend, branch to form mycelia. With maturation of mycelia, they will reproduce spores.[19] In general, mycelia and spores comprise colonies. For the colony from day 2 to 6, there were small qualities of mycelia initially, and then those mycelia grow away from the origin point (the center) of the colony. Finally, the colonies become round and expand. The colony size was indexed by the number of pixels. Figure 3 shows the growth curves of the fungus incubated on two nutritional media for colony size with inoculation day.

Colony growth of fungi could usually be divided into four phases: A lag phase, an exponential phase (logarithmic phase), a stationary phase and a decline phase.[21] The two growth curves in Fig. 3 illustrate the first three phases. As the pixel number

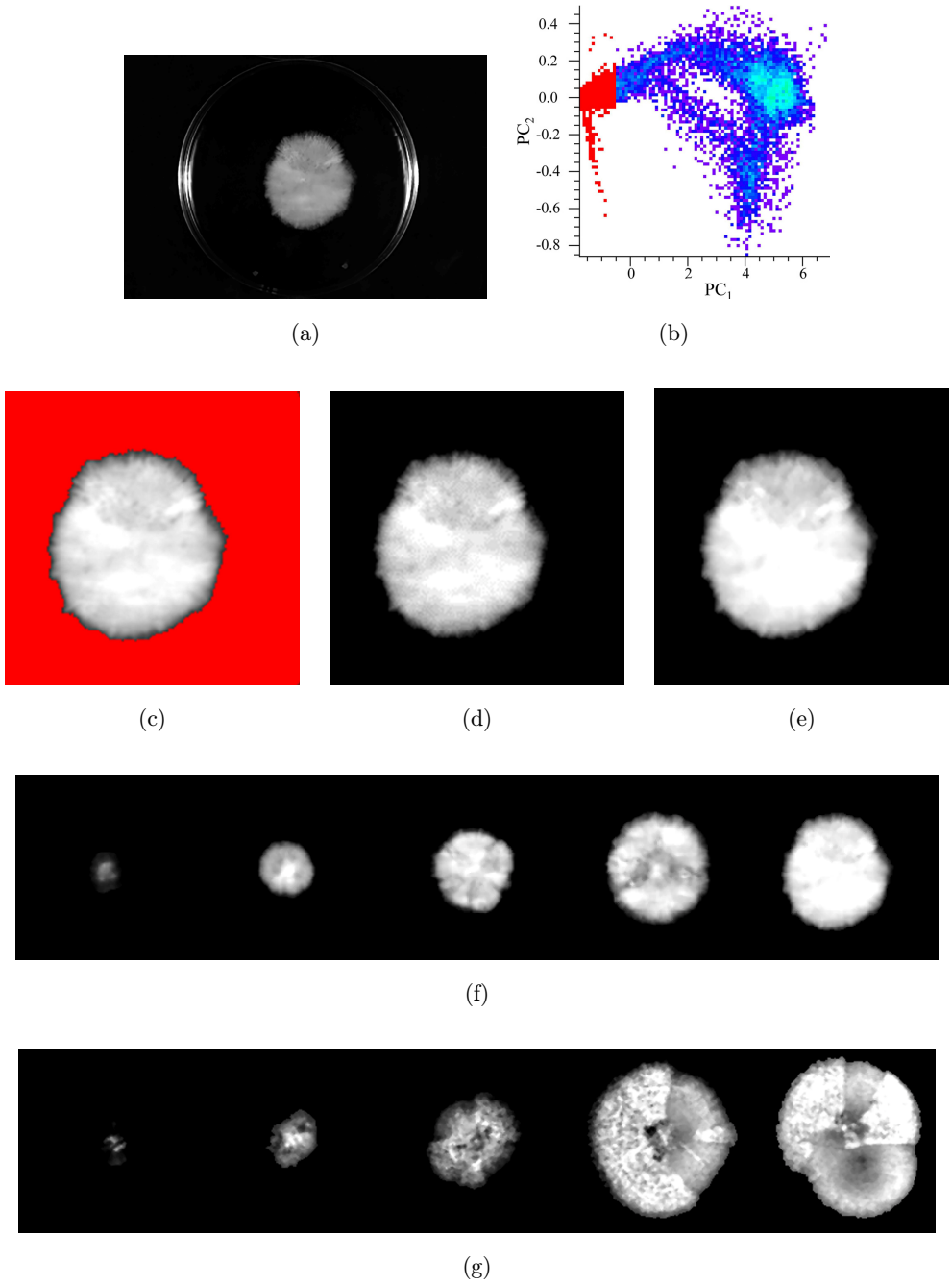

Fig. 2. An illustration of hyperspectral images preprocessing. (a) Gray image of colony incubated on RBM. (b) Score plot of PC_1 against PC_2. (c) Corresponding pixels of background. (d) Extracted colony. (e) Corrected colony image. (f) Colonies growing on RBM. (g) Colonies growing on MAM.

of the colony did not decrease on day 6 in this study, decline phase cannot be shown in the growth curves. From day 2 to day 3, it was observed that sparse mycelia started to appear and extend around the original inoculation point. However, the mycelial size grew slowly. Perhaps because mycelia need to adapt to the environment for germination.[22], it could be speculated that the colony was in the lag phase. After day 3, a sharp increase in the profiles indicated that the colony started to enter into the exponential phase. In this phase, mycelia were the most active and divided at the maximal rate, leading to colony growth radially with an exponential rate. The colonies reached stationary phase after day 5, in which, mycelia growth almost ceases and the cell density remains roughly constant.[23] Thus,

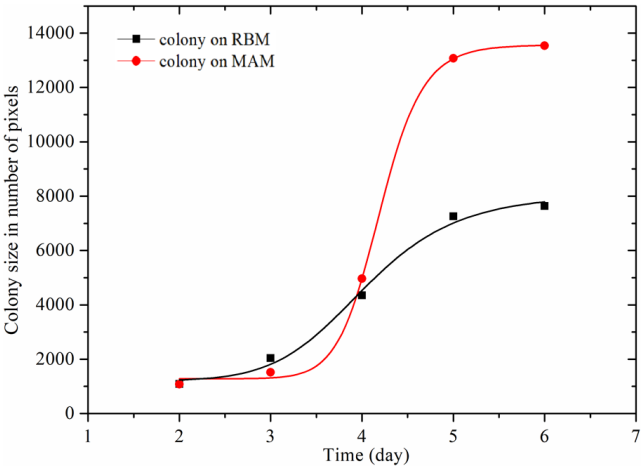

Fig. 3. Growth curves of colonies.

as the curves show in Fig. 3, the colony size increased little after day 5.

As the colony was primarily composed of mycelia consisting of a mass of branching, thread-like hyphae, the spectral signature of the colony would change over the incubation time. Therefore, the spectra of each colony were extracted and used. Just taking spectra of colonies incubated on RBM as an example to show the spectral change (Fig. 4(a)). The pattern of each mean spectra curve of the colony incubated on the same medium for different days was similar to each other. However, the reflectance increases significantly over the incubation time. The peaks and valleys on the spectrum curves became more and more obvious over the colony growing. These changes could be attributed to variation of morphology of the colony with cumulative incubation time, as aged colony was thicker than new colony, and the branched network of mycelia on aged colonies was denser than those on new colonies.

Moreover, there were some obvious peaks and valleys on the average spectrum curves, i.e., 1095, 1145, 1195, 1279, 1442, 1655, 1834 and 1929 nm. Among them, 1145 nm could be attributed to the second overtone of C–H in aromatic[24]; 1655 nm could be related to the C–H structure of CH_3Br; 1195 nm (C–H stretch second overtone, CH_3), 1279 nm (2 × C–H stretch + C–H deformation-CH_3), 1442 nm (O–H stretch), 1837 nm (O–H stretch + 2 × C–O stretch, cellulose) and 1929 nm (O–H stretch + HOH deformation combination, starch and cellulose), all associated with carbohydrates.[11,25] Gottlieb and Van Etten (1964)[26] concluded that the percentage of carbohydrates in the mycelium increased continually until it reached the late exponential phase and then decreased as the fungus entered the decline phase. The mycelium cell wall is exclusively comprised of polysaccharides. The number of mycelium cell walls will change with the growth of the colony,[27] leading to the varying in carbohydrates. Thus, those wavelengths that reflect the changes in different growth phases could be selected as significant bands. It should be noted that the key spectral wavelengths selected from the colonies cultured on MAM (Fig. 4(b)) were nearly identical to those on the RBM, which, on the other hand, verified the above judgment.

The morphology of a colony was modeled as a cone. Its density decreases gradually from the center to the edge.[28,29] If only using the spectra of the

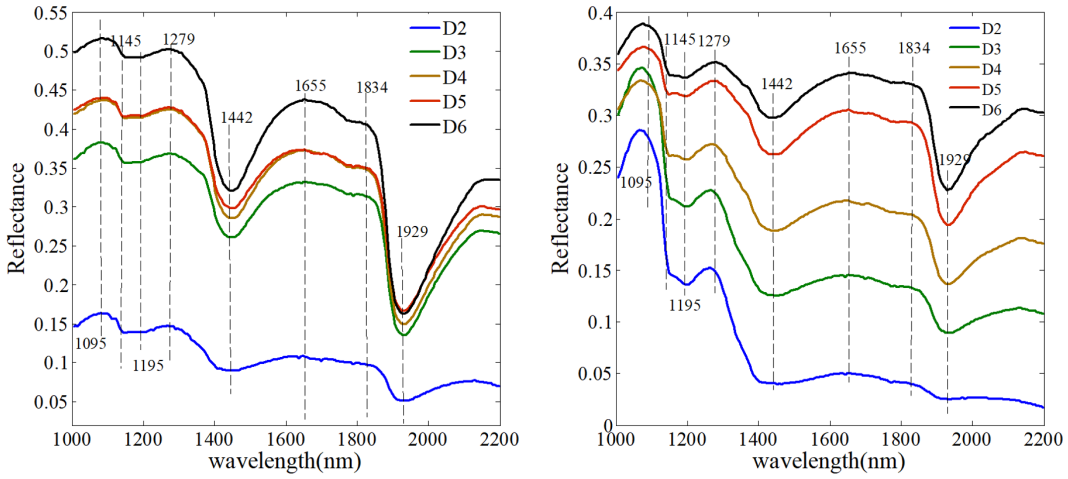

Fig. 4. Average spectra of each colony. (a) Average spectra of colonies on RBM. (b) Average spectra of colonies on MAM.

whole colony, it is insufficient to descript the mycelial distribution information. Therefore, spectral information of each pixel on colonies would be better for further colony growth evaluation.

3.3. *Identification of growth zones corresponding to different growth phases of fungal colony*

A colony generally grows radially outwards from the inoculation point. A series of fairy rings generate with the colony growing. Morphological studies of fungal colonies indicated that a mature colony on solid substrates could be divided into four morphological zones from outside to inside: extending zone, productive zone, fruiting zone and aged zone.[19] Among the four zones, old mycelia were in the center while the young were in the edge.[16] Mycelia growing in the same zone were assumed to have the same age.[19] The extending zone, in which mycelia increase in length, contributes to the extension of the colony. The productive zone next to the extending zone consists of a dense net of vegetative mycelia to support the growth of aerial hyphae. With the maturation of the mycelia, fruiting zone arises, in which reproductive structures appear and spores start to be produced. Finally, the center area of the colony germinates to the aged zone. As described by David *et al.* (2016),[30] mycelia differentiation of each zone is very evident in the morphological differentiation of fungal colonies and thus could be identified with the naked eye.

PCA was applied on the two mosaics comprised of the hyperspectral images of colonies, respectively, growing on RBM and MAM for 2–6 days. while computing PCA, all the background was removed to eliminate their interference. As the results were similar to each other, here we just showed the results for colonies on RBM. The variance contribution rates of the most important two PCs were 99.82% and 0.14%, individually. The score plot for PC_1 and PC_2 was explored, and a rough delineation of clusters in the direction of PC_1 was shown in Fig. 5(a). Based on morphology researches of Georgiou and Shuler (1986)[19] and the pixel clustering shown in Fig. 5(a), the pixels were divided into four parts (Fig. 5(b)). The classes were selected by dividing the pixels along with the axis of PC_1 in almost equal segments, and the dividing was done by starting with the low score value moving towards the high scores.[31] The classification result (Fig. 5(c)) was coincident with the growth zones divided by visual rating for the colony. Using the classified growth zones and pixel statistics of each zone (Fig. 5(d)) can give more details of the growth characteristics of the four growth zones corresponding to different growth phases.

In order to further elucidate the relationship between mycelium growth zones and growth phases, mycelial growth trend of every growth zone was developed and compared. Figure 5(c) showed the growth zones from the center toward the edge with the growth of the colonies. The four zones were inferred to correspond to the growth trend of the extending, productive, fruiting and aged zones.[11] As shown in Fig. 5(d), the blue, cyan, yellow and coral lines were the mycelia growth trends of the four zones during the six days. In day 2, colony was in lag phase, in which hyphae started to extend and branch gradually, leading to most of mycelia on the colony being in the extending (blue) and productive (cyan) zone. It was not mature enough to generate aged (coral) zone. Obviously, productive (cyan) zone was first located in the center of the colony, especially when mycelium growth was in its early stage. With the increasing of incubation time, more and older mycelia zones such as fruiting (yellow) and aged (coral) zones would occupy the center of the colony. In day 3, although colony was still in lag phase, mycelia extended outward little. The change in the of colony size was not obvious. However, most mycelia in extending (blue) and productive (cyan) zones transformed into fruiting (yellow) zone, and the fruiting (yellow) zone started to dominate the center area of the colony. After day 3, the colony started to enter into the exponential phase. The mycelia in the extending (blue) zone extended outward rapidly, and mycelia in the center continued to turn old. The number of pixels in each zone continued to increase rapidly until day 5 (Fig. 5(d)). At this point, the growth of colonies entered into a stationary phase, thus the colony size remains stable. Few new mycelia appeared, and the existing mycelia on it continued to be mature. The number of pixels in the extending (blue), productive (cyan) and fruiting (yellow) zones started to reduce and those in aged (coral) zone increased (Fig. 5(d)). Comprehensive analysis of the position, size and growth trend of every growth zone indicated that with the growth of the colony, mature growth zones emerged from the colony center, and the relative size of each zone on the colony and the growth

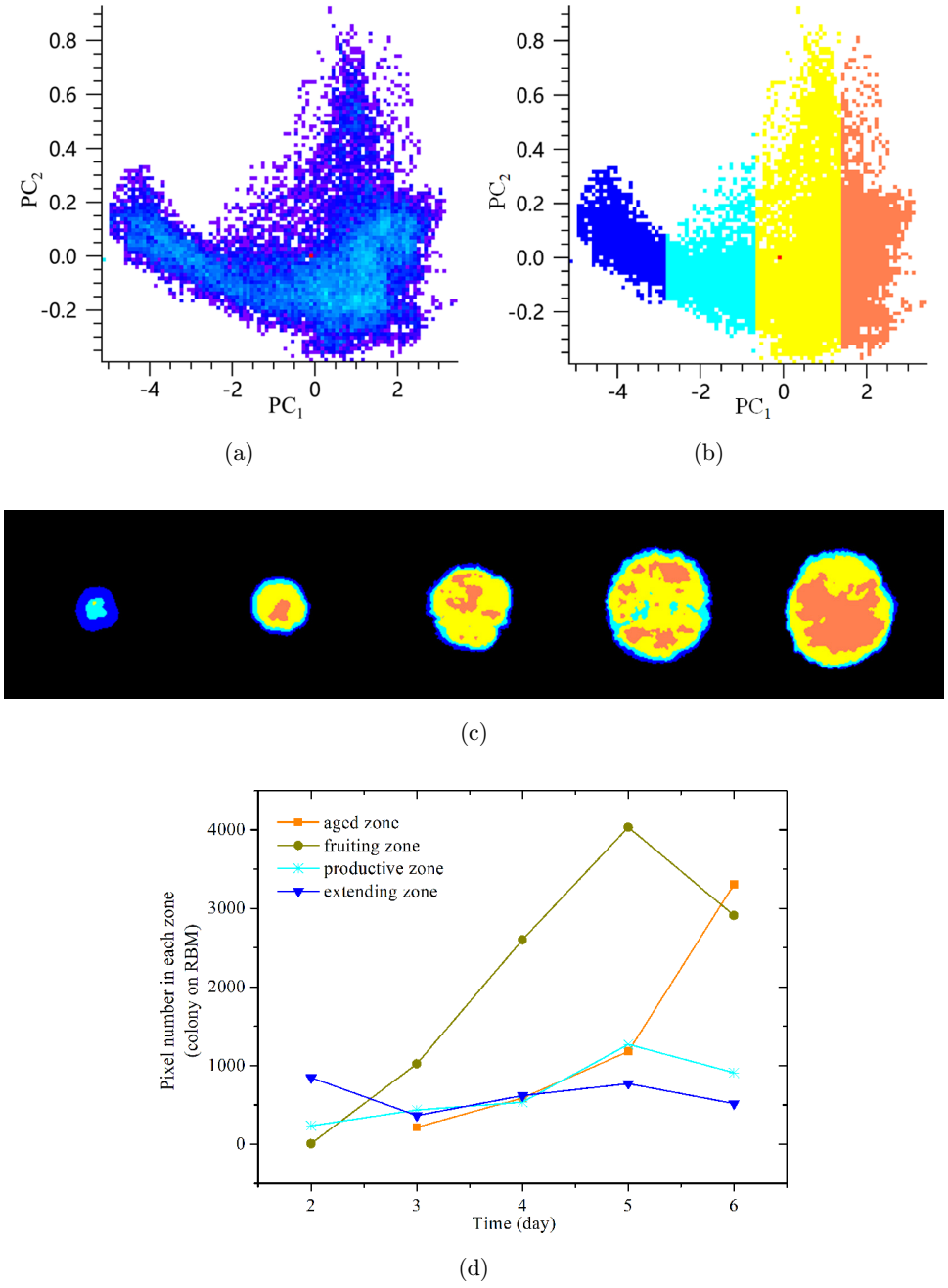

Fig. 5. Analysis of growth zones on colonies. (a) Score plot of PC_1 and PC_2. (b) Grouping pixels with similar score values along PC_1. (c) Projection of pixels groups onto image space. Blue is edge region; cyan is the area close to the edge; yellow is surrounding the center; coral is center of the colony. (d) Growth curve of each zone.

trends of each zone were different at varying growth phases.

3.4. *Acquisition of spectral signature of fungal colony growth zones*

The average spectral curves of the four zones were shown in Fig. 6(a). Taking an extreme example, the reflectance spectra of the aged mycelia in the center increased when compared with the young mycelia in the edge zones, and the peaks and valleys on the spectra of the center were more obvious than those of the mycelia on the edge. By the way, these were consistent with the trends of the mean spectra of the whole colony over the incubation time. The differences of spectra in the center and edge may be

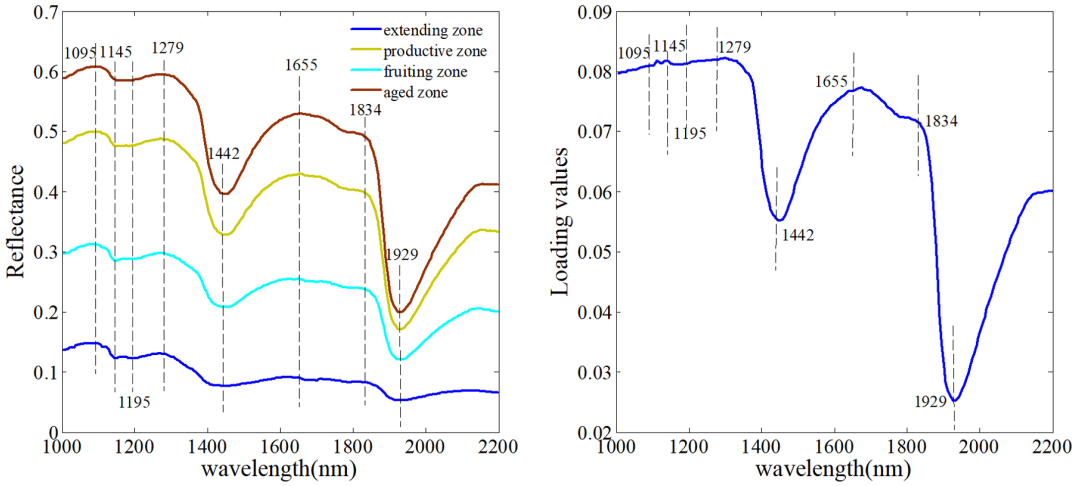

Fig. 6. Characteristic wavelengths selection. (a) Average spectra of each zone. (b) Loading plot of PC_1.

caused by the density and height of mycelia. Mycelia in center zones were denser than those in edge zones, and the height of mycelia decreased from center to edge.[32] All peaks and valleys on the average spectra of each zone also coincided with those selected from average spectra of whole colonies (1095, 1145, 1195, 1279, 1442, 1655, 1834 and 1929 nm). Furthermore, as shown in the loading plot of PC_1 (Fig. 6(b)), the eight wavelengths also contained larger weight coefficients, which were associated with biochemical changes during growth of the fungus. It was reported that more cell wall substance existed in the center region compared with in edge region. The wavelengths of 1195, 1279, 1442, 1837 and 1929 nm all correspond to carbohydrates which are the major components of fungal cell wall. Thus, those wavelengths could be taken as the feature parameters to identify growth characteristics of the fungus colony. Similar results were found for the colonies growing on MAM.

In addition, an SVM classification model based on the spectra at these characteristic wavelengths (1095, 1145, 1195, 1279, 1442 1655, 1834 and 1929 nm) for identification of each growth zone on colonies was built. Because of the clear classification results of PCA (Fig. 5(c)), the pixels selected according to PC_1 score were used as reference values of the model. As pixels in each zone were taken as samples to train the model, there were enough pixel samples to allow the selection of calibration and validation set. For example, the numbers of pixels were 2367, 2858, 9621 and 4103 in blue, cyan, yellow and coral region, respectively. Two-thirds of the pixels in each zone were selected as calibration set, and the rest were taken as validation set. In the present case, radial basis function (RBF) was chosen as kernel function of SVM, and different parameters were optimized by grid search technique. The performance of the classification model was evaluated by the classification accuracies of calibration and validation set and the accuracies got by comparing the results with PC_1 score classification results (Fig. 5(c)). The classification results for calibration and validation set were 99.66% and 99.65% for colonies on RBM, and 99.71% and 99.55% for colonies on MAM respectively. For the extending, productive, fruiting and aged zone, the classification accuracies were 99.77%, 99.35%, 99.75% and 99.60% for colonies on RBM, while the classification accuracies were 99.77%, 99.39%, 99.31% and 98.22% for colonies on the MAM. In order to show the classification quality visually, the predictive results of the two sets were refolded to form a prediction image (upper row of Figs. 7(a) and 7(b)). These results indicate that the growth characteristics for the colonies incubated on both RBM and MAM can be described by those eight characteristic wavelengths.

To further test the effect of SVM model on classifying the growth zones of colonies, two independent validation mosaics which were composed of images of colonies incubated for 2–6 days on RBM and MAM, respectively, were prepared. Those colonies were inoculated and incubated in the same sequence and condition as the colonies used for SVM model establishment. Prediction image of the

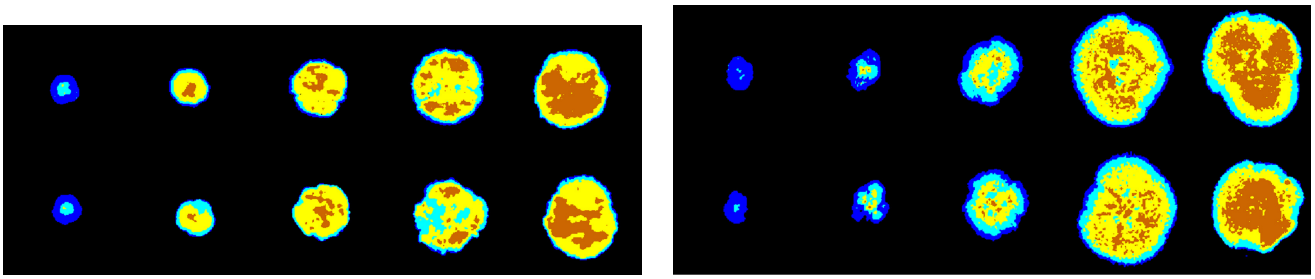

(a) (b)

Fig. 7. Prediction image of growth zones on colonies. (a) Prediction image of growth zones on colonies incubated on RBM. (b) Prediction image of growth zones on colonies incubated on MAM. (Classification based on the training data is in the upper row, and the bottom row is the classification result of the independent validation data).

independent validation mosaics group were also shown in button row of Figs. 7(a) and 7(b), respectively. The prediction image of the model training image (upper row of Fig. 7) were similar to the results got by PC score plot (Fig. 5(c)). The mature mycelia were in the center of the colonies and their size was becoming greater and greater with growing time. The neonatal mycelia were at the edge of colonies, and it radiated outward. All results further verified that, using those characteristic wavelengths only was feasible to describe the growth characteristic of the colonies.

3.5. *Feature parameter acquisition of A. parasiticus inoculated on different media*

Hyperspectral images of colonies incubated on the two media for 6th days were used to form a single mosaic (Fig. 8(a)), as the colonies already were in the stationary growth phase. Figure 8(a) shows that the colony growing on RBM was villiform with a smooth surface; while the colony growing on MAM had a rough surface. Thus, the spectral signature of the colony incubated on the two media may be different. However, in fact, although Fig. 8(b) shows that there was an obvious difference in reflectance, the spectra trends of the colonies growing on RBM and MAM were generally consistent and individual peaks on the two spectra also sowed a good coincidence.

PCA was further applied on the mosaic. During calculation, all the background pixels were removed and only the colony pixels were involved in computing. The score plot of PC_2 and PC_3 was shown in Fig. 8(c). It shows a clear delineation of two clusters potentially indicating the colony incubated on RBM and MAM, respectively. A classification description of the clusters was shown in Fig. 8(d), where the classes were made by polygon marking. Then the classification image was acquired by projecting the selected classes onto PC_1 score image (Fig. 8(e)). The maroon and blue pixels, respectively, correspond to the colonies incubated on RBM and MAM. This indicates that PC_2 and PC_3 play an important role in identifying fungus incubated on different media.

As on the score plot of PC_2 and PC_3, the pixels of colonies on different media could generate two obvious clusters. Thus, PC_2 and PC_3 could reflect the difference of the colonies on the two media. In order to find the optical parameters used to differentiate a fungus incubated on different media, characteristic wavelengths were explored. The loadings of PC_2 and PC_3 were shown in Fig. 8(f). Those wavelengths with larger absolute coefficients in each PC were considered to play an important role in representing the corresponding PC.[33] All the peaks and valleys (1067, 1195, 1279, 1369, 1459, 1694, 1834 and 1929 nm) of the loading line plots of PC_2 and PC_3 were selected as characteristic wavelengths. Among them, 1067 nm was near 1065 nm which was ascribed to the O–H structure of water. 1369 nm was mainly associated with C–H of $ArCH_3$. 1459 nm was related to the N–H of urea. 1694 nm was mainly associated with C–H in CH_3. 1834 nm and 1929 nm were associated with carbohydrates, which are also peaks on the average spectra of the whole colony. Thus, we conclude that those wavelengths can be selected as characteristic wavelengths to identify the fungi inoculated and incubated on different media.

Similar to the growth zone classification model, a new SVM classification model was calibrated to identify the colony incubated on RBM and MAM

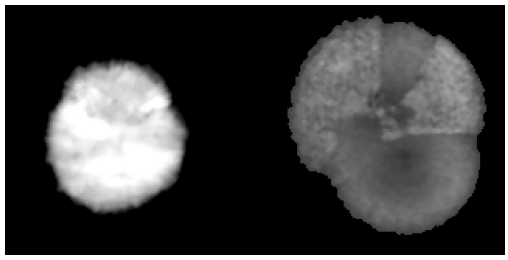

(a)

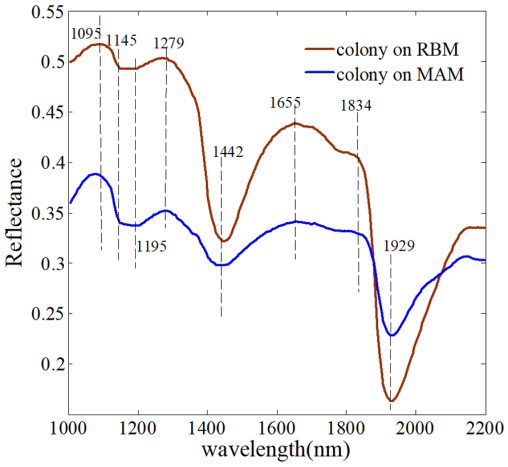

(b)

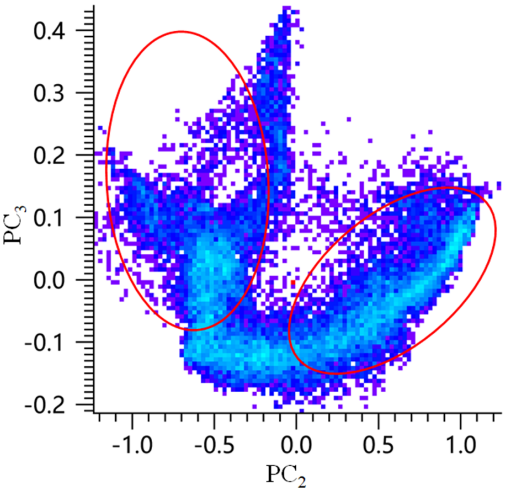

(c)

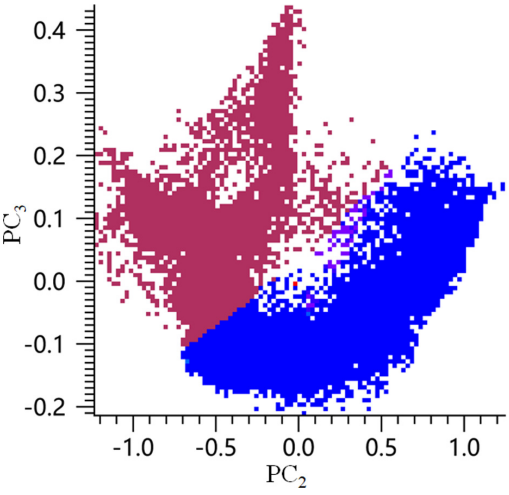

(d)

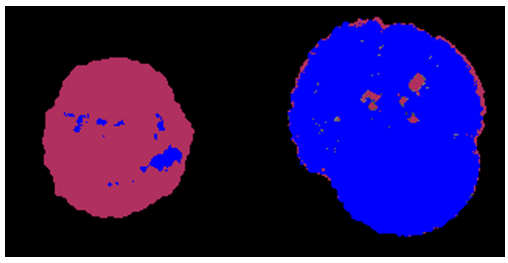

(e)

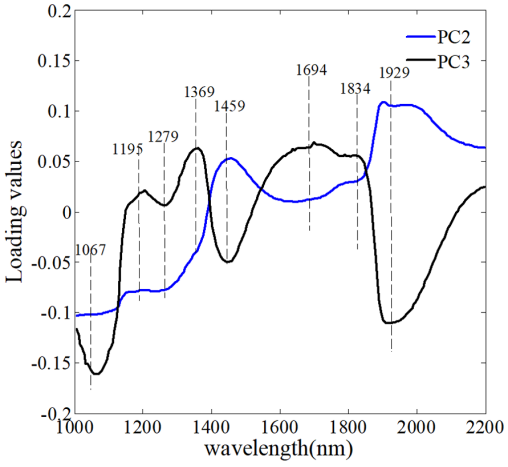

(f)

Fig. 8. Analysis of colonies on different media. (a) Gray image of the mosaic. Colony grown on RBM was on the left, and colony on MAM was on right. (b) Average spectra of each colony. (c) Score plot of PC_2 and PC_3. (d) Two identified clusters. (e) Classification projected onto the score image. (f) Loading line plot of PC_2 and PC_3.

for 6 days, respectively. All the pixels of the two colonies growing for 6 days were taken as samples. Two-third pixels in each colony were selected as calibration set, and the rest constituted the validation set. The spectra at those characteristic wavelengths of 1067, 1195, 1279, 1369, 1459, 1694, 1834 and 1929 nm were selected as input of the SVM classifier. In this model, RBF kernel function was used, and different parameters were also optimized by grid search technique. The classification accuracies for calibration and validation set were 100.00% and 99.99%. For each colony, the classification results for the pixels of colony on RBM reached 99.99%, and for the pixels of colony on MAM reached 100.00%. The prediction image of those colonies was shown in upper row of Fig. 9.

Finally, mosaic of colonies incubated on different media for 5th days were used as an independent validation data. Similarly, spectra at characteristic wavelengths were taken as input of the SVM classification model. Based on the classification results, the image of the independent validation data was redrawn in button row of Fig. 9. The maroon pixel was the colony incubated on RBM, and the blue one represented the pixels classified to the colony grown on MAM. Thus, the colonies incubated on different media not only can be identified by the PC_2 and PC_3, but also can be differentiated by the selected characteristic wavelengths.

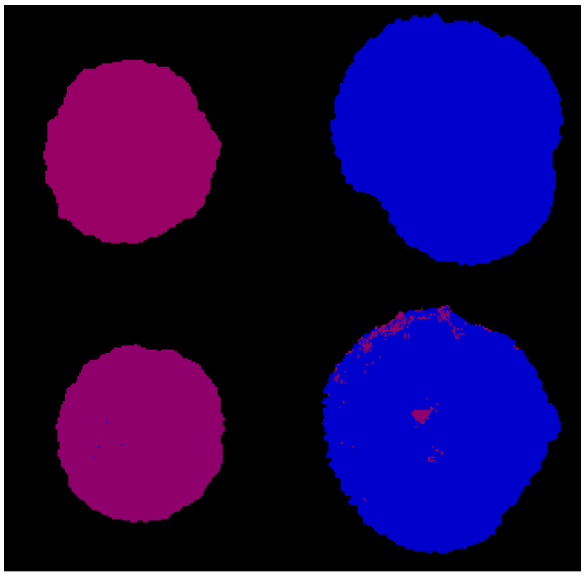

Fig. 9. Prediction image for colonies on different media (Classification based on the training data is in the upper row, and the bottom row is the classification result of the independent validation data).

4. Conclusions

The growth characteristics of *Aspergillus parasiticus* incubated on two culture media using shortwave infrared hyperspectral imaging with wavelength range from 1000 to 2500 nm were examined in the current study. The main conclusions are:

(1) SWIR hyperspectral imaging could be used to investigate growth phases and growth zones of the growing colonies. The lag, exponential and stationary phases during the colony growth were clearly identified through the comparison of colony pixel number in the gray image. The extending, productive, fruiting and aged zones on colonies were substantially differentiated according to the PC_1 score value in the score plot of PC_1 and PC_2. Average spectra of colonies incubated on the same medium for different durations and average spectra of different growth zones on colonies have a unique shape, and their reflectance values increased and the peaks become obvious with the prolonged incubation time and maturation of colonies, respectively. Eight wavelengths (1095, 1145, 1195, 1279, 1442 1655, 1834 and 1929 nm) located on the peaks of PC_1 loading plot and the average spectra of each colony as well as each growth zone were identified as the feature signatures of the fungal colony growth.

(2) Feature parameters acquired from SWIR hyperspectral images could be used to differentiate *A. parasiticus* inoculated on different media. Two distinct clusters on the score plot of PC_2 and PC_3 corresponded to the colony incubated on RBM and MAM media, respectively. Eight wavelengths (1067, 1195, 1279, 1369, 1459, 1694, 1834 and 1929 nm) located on the peaks of loading of PC_2 and PC_3 were identified as characteristic wavelengths.

(3) SVM classification models built based on selected characteristic wavelengths could identify different growth zones on colonies and colonies incubated on different media. The classification accuracies of the SVM model developed based on the seven characteristic wavelengths of the four growth zones (from outer to inner zones) on the growing colonies were 99.77%, 99.35%, 99.75% and 99.60% of colonies on the RBM and 99.77%, 99.39%, 99.31% and 98.22% for colonies on the MAM. The classification accuracies of the SVM model developed based on the six wavelengths for pixels of colony incubated for 6 days on the RBM and MAM medium were 100.00% and 99.99%, respectively.

In general, the results illustrated that hyperspectral imaging is a useful tool to analyze the growth characteristics of *Aspergillus parasiticus.* However, this study has only involved *A. parasiticus* only grown on rose bengal media and maize ager media. In order to further investigate the ability of hyperspectral imaging in analyzing the growth of fungi, more kinds of fungi grown on different media should be carried out gradually.

Conflicts of Interest

The authors declare no conflict of interest.

Acknowledgments

This work was supported financially by the National Natural Science Foundation of China (No. 31772062) and Gannan Camellia Industry Development and Innovative Center Open Fund (Grant No. YK201610).

References

1. H. Palacios-Cabrera, M. H. Taniwaki, J. M. Hashimoto, H. C. D. Menezes, "Growth of Aspergillus ochraceus, A. carbonarius and *A. niger* on culture media at different water activities and temperatures," *Braz. J. Microbiol.* **36**(1), 24–28 (2005).
2. S. P. Kale, J. W. Cary, D. Bhatnagar, J. W. Bennett, "Characterization of experimentally induced, nonaflatoxigenic variant strains of Aspergillus parasiticus," *Appl. Environ. Microbiol.* **62**(9), 3399–3404 (1996).
3. M. E. Cawood, W. C. Gelderblom, R. Vleggaar, Y. Behrend, P. G. Thiel, W. F. Marasas, "Isolation of the fumonisin mycotoxins: A quantitative approach," *J. Agric. Food Chem.* **39**(11), 1958–1962 (1991).
4. Y. Sun, X. Gu, Z. Wang, Y. Huang, Y. Wei, M. Zhang, T. Kang, L. Pan, "Growth simulation and discrimination of Botrytis Cinerea, Rhizopus Stolonifer and Colletotrichum Acutatum using hyperspectral reflectance imaging," *PloS one* **10**(12), e0143400 (2015).
5. S. E. Matcham, B. R. Jordan, D. A. Wood, "Estimation of fungal biomass in a solid substrate by three independent methods," *Appl. Microbiol. Biotechnol.* **21**(1), 108–112 (1985).
6. L. Edelstein, L. A. Segel, "Growth and metabolism in mycelial fungi," *J. Theor. Biol.* **104**(2), 187–210 (1983).
7. G. Sharma, "Influence of culture media on growth, colony character and sporulation of fungi isolated from decaying vegetable wastes," *J. Yeast Fungal Res.* **1**(8), 157–164 (2010).
8. H. Kalkan, P. Beriat, Y. Yardimci, T. C. Pearson, "Detection of contaminated hazelnuts and ground red chili pepper flakes by multispectral imaging," *Comput. Electron. Agr.* **77**(1), 28–34 (2011).
9. K. Dégardin, A. Guillemain, N. V. Guerreiro, Y. Roggo, "Near infrared spectroscopy for counterfeit detection using a large database of pharmaceutical tablets," *J. Pharm. Biomed. Anal.* **128**, 89–97. (2016).
10. P. J. Williams, P. Geladi, T. J. Britz, M. Manley, "Near-infrared (NIR) hyperspectral imaging and multivariate image analysis to study growth characteristics and differences between species and strains of members of the genus Fusarium," *Anal. Bioanal. Chem.* **404**(6–7), 1759–1769 (2012a).
11. P. J. Williams, P. Geladi, T. J. Britz, M. Manley, "Growth characteristics of three Fusarium species evaluated by near-infrared hyperspectral imaging and multivariate image analysis," *Appl. Microbiol. Biotechnol.* **96**(3), 803–813 (2012b).
12. J. Jin, L. Tang, Z. Hruska, H. Yao, "Classification of toxigenic and atoxigenic strains of Aspergillus flavus with hyperspectral imaging," *Comput. Electron. Agr.* **69**(2), 158–164 (2009).
13. H. Yao, Z. Hruska, R. Kincaid, R. L. Brown, T. E. Cleveland, "Differentiation of toxigenic fungi using hyperspectral imagery," *Sens. Instrumen. Food Qual.* **2**(3), 215–224 (2008).
14. P. J. Williams, S. Kucheryavskiy, "Classification of maize kernels using NIR hyperspectral imaging," *Food Chem.* **209**, 131–138 (2016).
15. T. L. Kammies, M. Manley, P. A. Gouws, P. J. Williams, "Differentiation of foodborne bacteria using NIR hyperspectral imaging and multivariate data analysis," *Appl. Microbiol. Biotechnol.* **100**(21), 9305–9320 (2016).
16. M. Kamruzzaman, G. ElMasry, D. W. Sun, P. Allen, "Application of NIR hyperspectral imaging for discrimination of lamb muscles," *J. Food Eng.* **104**(3), 332–340 (2011).
17. F. Melgani, L. Bruzzone, "Classification of hyperspectral remote sensing images with support vector machines," *IEEE Trans. Geosci. Electron.* **42**(8), 1778–1790 (2004).
18. P. Williams, M. Manley, G. Fox, P. Geladi, "Indirect detection of fusarium verticillioides in maize (zea maize l.) kernels by nir hyperspectral imaging," *J. Near Infrared Spectrosc.* **18**(1), 49–58 (2010).
19. G. Georgiou, M. L. Shuler, "A computer model for the growth and differentiation of a fungal colony on solid substrate," *Biotechnol. Bioeng.* **28**(3), 405–416 (1986).

20. G. Steinberg, "Hyphal growth: A tale of motors, lipids, and the Spitzenkörper," *Eukaryotic cell* **6**(3), 351–360 (2007).
21. A. P. J. Trinci, "A kinetic study of the growth of Aspergillus nidulans and other fungi," *Microbiol.* **57**(1), 11–24 (1969).
22. M. Gougouli, K. P. Koutsoumanis, "Modelling growth of Penicillium expansum and Aspergillus niger at constant and fluctuating temperature conditions," *Int. J. Food Microbiol.* **140**(2) 254–262 (2010).
23. S. Gao, G. D. Lewis, M. Ashokkumar, Y. Hemar, "Inactivation of microorganisms by low-frequency high-power ultrasound: Effect of growth phase and capsule properties of the bacteria," *Ultrason. Sonochem.* **21**(1), 446–453 (2014).
24. D. A. Burns, E. W. Ciurczak, Eds., Handbook of Near-Infrared Analysis (CRC Press, 2007), pp. 356–357.
25. J. Workman Jr., L. Weyer, *Practical Guide to Interpretive Near-Infrared Spectroscopy*, CRC Press (2007).
26. D. Gottlieb, J. L. Van Etten, "Biochemical changes during the growth of fungi I. Nitrogen compounds and carbohydrate changes in penicillium atrovenetum," *J. Bacteriol.* **88**(1), 114–121 (1964).
27. A. Beauvais, T. Fontaine, V. Aimanianda, J. P. Latgé, "Aspergillus cell wall and biofilm," *Mycopathologia* **178**(5–6), 371 (2014).
28. D. R. Gifford, S. E. Schoustra, "Modelling colony population growth in the filamentous fungus Aspergillus nidulans," *J. Theor. Biol.* **320**, 124–130 (2013).
29. T. H. Adams, J. K. Wieser, J. H. Yu, "Asexual sporulation in Aspergillus nidulans," *Microbiol. Mol. Biol. Rev.* **62**(1), 35–54 (1998).
30. M. David, D. R. Geoffrey, P. J. T. Anthony, *21st Century Guidebook to Fungi* (Cambridge University Press, 2016), http://www. davidmoore.org.uk/ 21st_Century_Guidebook_to_Fungi_PLATINUM/ Ch04 06.htm.
31. M. Manley, G. Du Toit, P. Geladi, "Tracking diffusion of conditioning water in single wheat kernels of different hardnesses by near infrared hyperspectral imaging," *Anal. Chim. Acta* **686**(1-2), 64–75 (2011).
32. J. W. Wimpenny, "The growth and form of bacterial colonies," *Microbiol.* **114**(2), 483–486 (1979).
33. J. Jiang, X. Qiao, R. He, "Use of Near-Infrared hyperspectral images to identify moldy peanuts," *J. Food Eng.* **169**, 284–290 (2016).